Proceedings of The Canadian Society for Mechanical Engineering International Congress 2018
CSME International Congress 2018
May 27-30, 2018, Toronto, On, Canada

3D PRINTING OF METALLIC STRUCTURES FROM A GREEN INK

Chao Xu, Louis Laberge Lebel, Daniel Therriault*
Mechanical engineering department
Polytechnique Montreal
Montreal, Canada
Daniel.therriault@polymtl.ca

Arslane Bouchemit, Gilles L'Espérance
Metallurgy engineering department
Polytechnique Montreal
Montreal, Canada

Abstract—A green metallic ink is developed for 3D printing of metallic structures featuring high mechanical and electrical performances. The metallic ink consists of steel micro powders and a water-based chitosan/acetic acid polymer solution which replaces the previously used toxic polylactic acid (PLA)/dichloromethane (DCM) polymer solution. The optimized ink is printed at room temperature to build a metal/polymer hybrid structure. While printing, a fan is used to blow air over the ink filament upon extrusion to accelerate the solvent evaporation and shorten the solidification time, which significantly reduces the sagging and deformation. After a drying period at ambient conditions, the as-printed structure is then thermally treated using a furnace. The polymer binder is decomposed and the metal powders are sintered, resulting in a strong metallic structure. Melted copper is infiltrated into the sintered structure to achieve a fully dense metal/metal hybrid structure. The sintered structure exhibits high stiffness (205 GPa), electrical conductivity (9×10^5 S/m) and low filament porosity (7%).

Keywords: 3D printing, metallic ink, environment-friendly, metallic structures, secondary metal infiltration

I. INTRODUCTION

Recently, 3D printing approaches have been developed to fabricate diverse metallic structures.[1-3] They offer many advantages such as more design flexibility, time efficient and less material waste over traditional metal manufacturing methods (e.g., machining). 3D printed metallic structures are applied in many fields such as medical [4-5], energy storage[6-7], sensors[8-9], and microelectronics[10-11]. Powder-bed approaches like selective laser sintering/melting (SLS/SLM) are mature, commercialized and progressively more widely used. These approaches are based on fine metal micro powders that are evenly spread out in a powder bed. A high-intensity laser is used to selectively fuse them to build layer-by-layer 3D structures.[12] However, the intense laser system is very costly and is a potential safety issue for the operator. In addition, the repeated scanning of the laser beam results in excessive material powder oxidation, loss of alloying elements and dramatical temperature change (which causes residual stresses and defects).[13-14]

To overcome these shortcomings, solvent-cast 3D printing (SC-3DP) is proposed, which combines room-temperature 3D printing and subsequent thermal treatments. This extrusion-based printing method employs an viscous metallic suspension consisting of metal powders, polymer binder and volatile solvent, referred as the ink.[15] Under applied pressure, the metallic ink is extruded from a fine nozzle and deposited on a substrate in a layer-by-layer fashion. Post the filament extrusion, the volatile solvent quickly evaporates and the ink turns into solid state. The as-printed object is a metal/polymer hybrid structure which is then thermally treated to burn the polymer binder and to sinter the metal powders, resulting in a fully metallic structure.[15] Many researchers adapted this approach to fabricate various 3D metallic structures featuring complex 3D geometries and high mechanical and electrical performances. [15-17] Although this type of process is simple and practical, it generally uses a volatile and toxic solvent (e.g., dichloromethane (DCM)), as the polymer binder solvent. We developed a nontoxic metallic ink consisting of chitosan, acetic acid, deionized water and metal powders. Chitosan is a biocompatible polymer which is dissolved in acetic acid aqueous solution as a viscous hydrogel. The metal powders are evenly dispersed in the hydrogel, resulting in a metallic suspension (Fig.1a). The metallic ink is extruded under a certain pressure and deposited on a substrate using a 3-axis deposition robot. After extrusion, the solvent (acetic acid and water) evaporates, whereas the chitosan and metal powders are left in the ink filament. Fig. 1b shows the schematic of subsequent thermal treatments. The as-printed sample is first sintered at 1165°C in order to thermally decompose the chitosan and sinter the metal powder. The sintered sample is a slightly porous metallic structure. To obtain a fully dense metallic structure, the sintered sample can be heated at 1120°C with a piece of copper placed on top of it. At this temperature, the melted copper can infiltrate the sintered structure to achieve a metal/metal hybrid structure.

II. RESULTS AND DISCUSSION

Fig. 2 shows an optical image and SEM images of the as-printed, sintered and copper infiltrated scaffolds printed with a tapered nozzle (tip inner diameter = 50 μm) at a printing speed

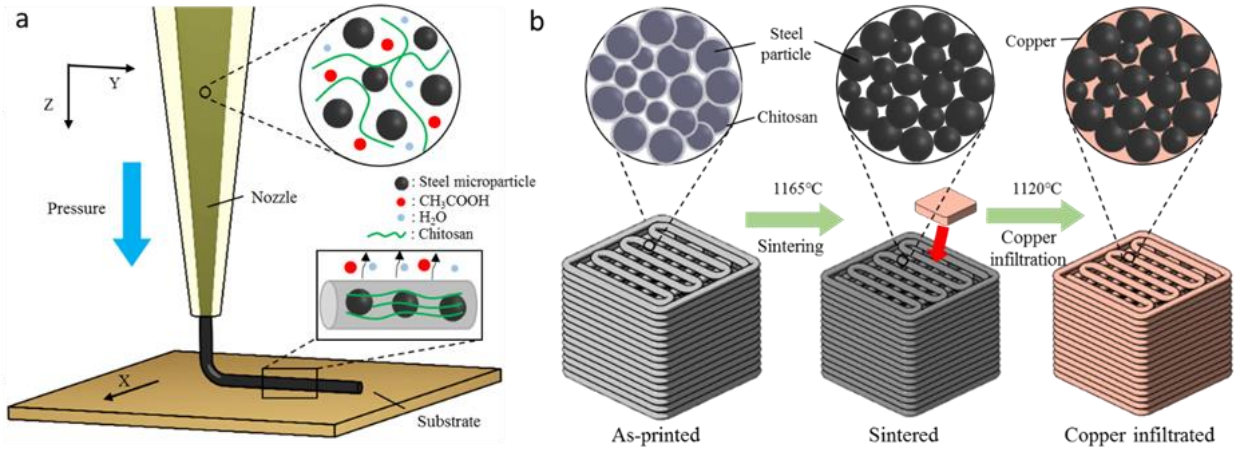

Fig. 1. Schematic of the fabrication process of a 3D metallic scaffold combining the following steps. (a) Solvent-cast 3D printing of a metallic ink consisting of steel microparticles and chitosan/acetic acid polymer solution. The metallic ink is loaded in a syringe and extruded through a micro nozzle under a certain pressure at room temperature. The solvent content evaporates upon extrusion assisted by an airflow. (b) Subsequent thermal treatments: the dried as-printed sample is thermally treated. The polymer is decomposed and the steel particles are sintered. Melted copper is infiltrated into the sintered structures to achieve a fully dense metallic structure.

of 7 mm/s. The three types of scaffolds are placed on a Canadian dollar. The as-printed scaffold has a dark gray color because the steel powders are covered by chitosan. After sintering, chitosan is removed and steel powders are brought closer. The sintered scaffold turns into light grey and shrinks in size. The copper infiltrated scaffold turns to brown red due to the appearance of copper. There are no significant shape distortion or oxidation occurred to the sintered and copper infiltrated scaffolds. The SEM images of the as-printed scaffold shows that steel powders are covered and bound by the polymer binder, chitosan (Fig. 2a). Before sintering, a debinding step is performed to remove the chitosan within the structure. After debinding, the structure integrity is held by the friction forces between the steel powders. The steel powders are sintered at a temperature slightly lower than their melting point. The powders are connected through the appearance of necks between them. The size and amount of the necks increase gradually, which densifies the sintered structure and reduces the pores. In the sintered scaffold (Fig. 2b), the chitosan is completely removed and the steel powders are directly connected with each other through the necks. For the copper infiltration, a piece of copper is placed on top of the sintered structures inside the oven. The sample is heated at 1120 ℃. This temperature is higher than the melting point of copper (1085 ℃), but lower than the previously used sintering temperature. Mainly driven by capillary forces, the melted copper fills the pores within the filaments of the structure (Fig. 2c).

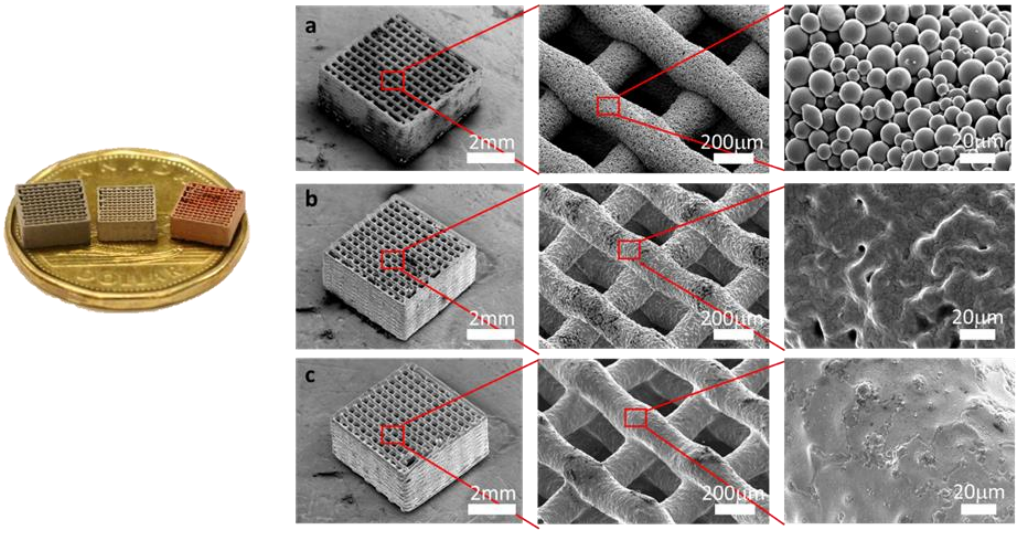

Fig. 2. Optical and SEM images of the scaffolds printed using a tapered nozzle (tip inner diameter = 50 µm) at a printing speed of 7 mm/s, (a) as-printed, (b) sintered, (c) copper infiltrated, and their close-up views.

The linear size reduction, filament porosity, electrical conductivity and mechanical properties of as-printed, sintered and copper infiltrated samples are characterized (Fig. 3). The samples have size variations in every stage compared to the designed size. It is caused by the swelling upon extrusion, solvent evaporation, debinding, sintering and copper infiltration. The linear size reduction is studied and the result is shown in Fig. 3a. The extruded ink filament swells due to the pressure drop and then shrinks as a result of the solvent evaporation. The dried as-printed sample has similar size as the designed one (>1% linear expansion). After debinding and sintering, the sintered structure shrinks by around 12% compared to designed size. The copper infiltrated sample exhibits less size reduction (~ 9% linear reduction) than the sintered one. The filament porosity of sintered samples is around 7% (Fig. 3b). After copper infiltration, the majority of the pores are filled by melted copper. The filament porosity of copper infiltrated samples is lower than 1%. The conductivity of sintered samples is around 9×10^5 S/m, which is 64% of that of the bulk material (Fig. 3c). As copper is more conductive than steel, the copper infiltrated sample presents an even higher conductivity of ~ 1.3×10^6 S/m. Fully dense sintered and copper infiltrated tensile bars, of which the cross section of the narrow part is $\approx 3.6 \times 1.6$ mm, are prepared for tensile test. It is carried out on a MTS Insight machine with a 50 kN load cell (MTS 569332-01) at a crosshead speed of 1 mm/min and using an extensometer (gauge length = 8 mm, MTS 632.26, C-20). Five specimens for each sample type are tested. The Young's modulus of sintered samples is around 205 GPa, which equals 95% of that of bulk material (Fig. 3d). After copper infiltration, the stiffness is slightly decreased, but the ductility and the ultimate tensile strength are significantly improved.

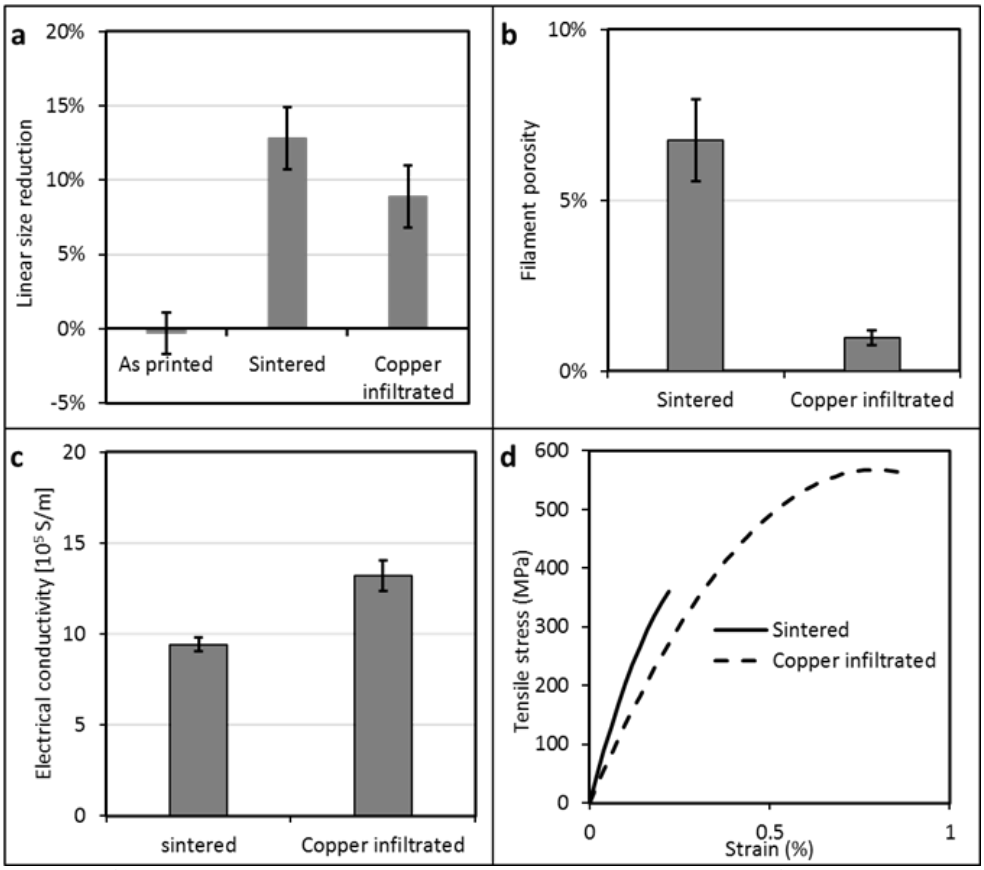

Fig. 3. (a) Linear size reduction, (b) filament porosity, (c) electrical conductivity and (d) mechanical properties of the as-printed, sintered and copper infiltrated samples

III. CONCLUSION

We developed an environmental metallic ink for SC-3D printing of highly dense metallic structures. The ink contains metal powders, biocompatible polymer binder and a nontoxic volatile solvent. Metallic and metal/metal hybrid structures are fabricated by subsequent thermal treatments. The linear size reduction, filament porosity, electrical conductivity and mechanical properties of the fabricated structures are characterized. The sintered structure has a Young's modulus close to that of the bulk material. The copper infiltrated structure exhibits less filament porosity, higher electrical conductivity and better ductility. The reported ink can replace the commonly used toxic ink to create 3D metallic structures for higher performances, lower environmental impact and more effective utilization of metallic materials.

ACKNOWLEDGMENT

The authors acknowledge the financial support from NSERC (Natural Sciences and Engineering Research Council of Canada, grant number: RGPIN 312568-2013) and Auto 21 of the Canadian Network of Centers of Excellence (NCE) program. A scholarship for Mr. Xu was also provided by the China scholarship Council (CSC) and the Fonds de recherche du Quebec - Nature et technologies (FRQNT).

REFERENCES

[1] Martin, John H., et al. "3D printing of high-strength aluminium alloys." Nature 549.7672 (2017): 365.

[2] Todd, Iain. "Metallurgy: No more tears for metal 3D printing." Nature 549.7672 (2017): 342.

[3] Gu, D. D., et al. "Laser additive manufacturing of metallic components: materials, processes and mechanisms." International materials reviews 57.3 (2012): 133-164.

[4] Elahinia, Mohammad H., et al. "Manufacturing and processing of NiTi implants: a review." Progress in materials science 57.5 (2012): 911-946.

[5] Wang, Xiaojian, et al. "Topological design and additive manufacturing of porous metals for bone scaffolds and orthopaedic implants: a review." Biomaterials 83 (2016): 127-141.

[6] Mendoza- Sánchez, Beatriz, and Yury Gogotsi. "Synthesis of Two- Dimensional Materials for Capacitive Energy Storage." Advanced Materials 28.29 (2016): 6104-6135.

[7] Jakus, Adam E., et al. "Metallic architectures from 3D- printed powder- based liquid inks." Advanced Functional Materials 25.45 (2015): 6985-6995.

[8] Song, Jun Hyuk, et al. "Surface- Embedded Stretchable Electrodes by Direct Printing and their Uses to Fabricate Ultrathin Vibration Sensors and Circuits for 3D Structures." Advanced Materials 29.43 (2017).

[9] Rim, You Seung, et al. "Recent progress in materials and devices toward printable and flexible sensors." Advanced Materials 28.22 (2016): 4415-4440.

[10] Boley, J. William, et al. "Direct writing of gallium- indium alloy for stretchable electronics." Advanced Functional Materials 24.23 (2014): 3501-3507.

[11] Dickey, Michael D. "Stretchable and Soft Electronics using Liquid Metals." Advanced Materials (2017).

[12] Farahani, Rouhollah D., Martine Dubé, and Daniel Therriault. "Three- dimensional printing of multifunctional nanocomposites: manufacturing techniques and applications." Advanced Materials 28.28 (2016): 5794-5821.

[13] Gong, Haijun, et al. "Influence of defects on mechanical properties of Ti–6Al–4V components produced by selective laser melting and electron beam melting." Materials & Design 86 (2015): 545-554.

[14] Olakanmi, E. O. T., R. F. Cochrane, and K. W. Dalgarno. "A review on selective laser sintering/melting (SLS/SLM) of aluminium alloy powders: Processing, microstructure, and properties." Progress in Materials Science 74 (2015): 401-477.

[15] Ahn, Bok Yeop, et al. "Printed origami structures." Advanced Materials 22.20 (2010): 2251-2254.

[16] Xu, Chao, et al. "Solvent-cast based metal 3D printing and secondary metallic infiltration." Journal of Materials Chemistry C 5.40 (2017): 10448-10455.

[17] Peng, Erwin, et al. "Ferrite-based soft and hard magnetic structures by extrusion free-forming." RSC Advances 7.43 (2017): 27128-27138.

[18]

